

# Identification of Different Vapors Using a Single Temperature Modulated Polymer Sensor With a Novel Signal Processing Technique

Takao Iwaki, James A. Covington, and Julian W. Gardner, *Senior Member, IEEE*

**Abstract**—This paper reports on a novel temperature modulation technique to improve the ability of a single carbon black/polymer resistive sensor to discriminate, identify and characterize environmental pollutants. Such a sensor can be low cost, low-power consumption, highly reliable, and thus ideal for indoor gas monitoring. Here, a carbon black/polyvinylpyrrolidone film was deposited onto an SOI-CMOS microhotplate. A novel temperature modulation technique is proposed that allows the detection of vapors using a single chemoresistor. Identification and quantification of water, methanol and ethanol vapors with different concentrations (water: 0–6000 ppm, methanol: 1360–5430 ppm and ethanol: 2270–9080 ppm) are shown.

**Index Terms**—Carbon black/polymer composite, gas sensor, microhotplate, temperature modulation.

## I. INTRODUCTION

AT PRESENT there is a considerable demand for portable, handheld gas or vapor monitors of pollutants. Although there has been some commercial success, the diversity of gases that cause air pollution makes it difficult to identify the species and to measure their concentration at low cost. For example, various types of volatile organic compounds (VOCs), such as formaldehyde, benzene, toluene, and xylene, emitted from sources inside buildings can cause indoor air pollution [1]. Furthermore, automobiles emit polluting gases such as carbon monoxide, nitrogen oxides, and, again, VOCs [2].

Currently, the gold standard for the identification and quantification of pollutants is using expensive analytical instruments, such as gas chromatographs, mass spectrometers and optical spectrometers. Research towards miniaturization of such instruments has been carried out (e.g., [3]), but the degree of miniaturization is limited by the high number of parts required to replicate the complicated operating principles. In practice, electrochemical sensors, catalytic bead pellistors and metal oxide resistive sensors are used to detect the different hazardous gases.

Manuscript received May 31, 2008; revised September 14, 2008; accepted September 22, 2008. Current version published February 25, 2009. This paper was presented at the 2007 IEEE Sensors Conference and was published in its proceedings. The associate editor coordinating the review of this paper and approving it for publication was Dr. Giorgio Sberveglieri.

T. Iwaki was with the School of Engineering, University of Warwick, Coventry CV4 7AL, UK. He is now with Denso Corporation, Aichi 470-0111, Japan (e-mail: TAKAO\_IWAKI@denso.co.jp).

J. A. Covington and J. W. Gardner are with the School of Engineering, University of Warwick, Coventry CV4 7AL, U.K. (e-mail: J.A.Covington@warwick.ac.uk; J.W.Gardner@warwick.ac.uk).

Color versions of one or more of the figures in this paper are available online at <http://ieeexplore.ieee.org>.

Digital Object Identifier 10.1109/JSEN.2008.2012238

They are still relatively expensive and/or require considerable power consumption.

Two other approaches for creating handheld gas detectors have been explored. One is to use an array of gas sensors with different sensing materials [4] and the other is to use temperature modulation of a single gas sensor [5], [6]. In the former case, by using an array, it is possible to detect, identify, and quantify different gases. For example, Severin *et al.* successfully demonstrated the identification and quantification of different vapors (e.g., eight types of single alcohol vapors) with an array comprising of 20 carbon black/polymer composite chemoresistors [4]. However, the main problem of this approach, when used for ubiquitous environmental gas monitors, is the cost; the development cost for 10–20 different types of chemical sensors with appropriate reliability is high. In the latter case, previous research on the temperature modulation of gas sensors has been carried out using metal oxide chemoresistors [5], [6]. Those reported have been successful in the identification and quantification of gases they tested. However, there is a major issue that requires resolving before commercialisation. Precalibration of the sensors is needed for not only single gases but also their mixtures with considering all the possible concentration combinations. This is because the response of metal oxide gas sensors is nonlinear in gas concentration and thus a simple superposition of the responses for different gases is problematic [7]. Suppose a sensor is sensitive to five different gases and measurements at just five different concentrations are required for each gas,  $5^5 = 3125$  premeasurements (covering all the possible combinations) have to be carried out for calibration.

We recently reported at a conference the concept of a novel gas sensing technique, which allows the identification and quantification of various vapors systematically (like analytical instruments) but using a single temperature modulated *polymer* sensor [8]. This paper describes in full, details of the proposed technique, covering the theoretical and experimental results to both single and complex mixtures.

## II. MODELING OF TRANSIENT CONDUCTANCE ASSOCIATED WITH A TEMPERATURE STEP IN A SINGLE VAPOR

A carbon black/polymer composite film comprises of an insulating polymer into which carbon black nanoparticles are dispersed to provide electrical pathways. When exposed to a vapor, the molecules (solute) diffuse (i.e., partition) into the film (solvent) causing it to swell. This swelling increases the average separation of the conducting nanoparticles and, thus, increases the electrical resistance of the film. Previous work has shown

that the change in electrical resistance is approximately proportional to the concentration of the vapor in air, i.e., it obeys Henry's adsorption law at low concentrations. In a linear solvation process, the concentration  $c$  of vapor molecules dissolved in the polymer is simply proportional to that in the vapor phase. The proportional constant or partition coefficient  $K(T)$  is defined as

$$K(T) = \frac{c_{\text{polymer}}(T)}{c_{\text{vapor}}} \quad (1)$$

where  $c_{\text{vapor}}$  is the vapor concentration in air and  $c_{\text{polymer}}(T)$  is its concentration in the polymer film held at temperature  $T$ .

It is well known that this partition coefficient is a function of temperature

$$\Delta H_0 = -RT \ln[K(T)] \quad (2)$$

where  $\Delta H_0$  is the standard enthalpy change for the interaction between the polymer and the vapor molecule, which is a constant specific to the system, and  $R$  is the gas constant [9]. Thus, if the temperature of the film increases from  $T_1$  to  $T_2$  (i.e.,  $T_1 < T_2$ ) under constant ambient vapor concentration, then the vapor concentration in the polymer decreases from  $c_{\text{polymer}}(T_1)$  to  $c_{\text{polymer}}(T_2)$ . In other words, vapor molecules have diffused out of the polymer and into the air as  $c_{\text{polymer}}(T_2)$  is smaller than  $c_{\text{polymer}}(T_1)$ . (Note: When the temperature is reduced from  $T_2$  to  $T_1$ , vapor molecules diffuse into the polymer from the air.) The diffusion process is governed by a diffusion coefficient of the vapor at temperature  $T_2$ , which is specific to the type of vapor and polymer. (Note: We assume that the diffusion takes place at  $T_2$ , i.e., that the temperature change is *quasi*-instantaneous.) We can use the behavior of the transient signals to identify different organic vapors in air.

To calculate this transient conductance for a step temperature change from  $T_1$  to  $T_2$ , we first assume that the diffusion of vapor into the polymer is a linear process and thus simply follows Fick's law [10]

$$\frac{\partial c(x,t)}{\partial t} = D_{T_2} \frac{\partial^2 c(x,t)}{\partial x^2} \quad (0 < x < h) \quad (3)$$

where  $c$  is the concentration of the vapor in the polymer,  $h$  is the thickness of the film. The initial concentration profile is uniform at  $T_1$

$$c(x,0) = c_{\text{polymer}}(T_1) \quad (0 < x < h). \quad (4a)$$

Boundary conditions are as follows:

$$c(0,t) = c_{\text{polymer}}(T_2) \quad (4b)$$

$$\frac{\partial c}{\partial x} = 0 \quad (x = h). \quad (4c)$$

Equation (4b) shows that the concentration at the surface of the polymer is independent of time and a constant value of  $c_{\text{polymer}}(T_2)$ , and (4c) expresses the condition where there is no flux through the substrate on which the film lies, i.e., it is impermeable. The analytical solution to the model is sketched out in Fig. 1.

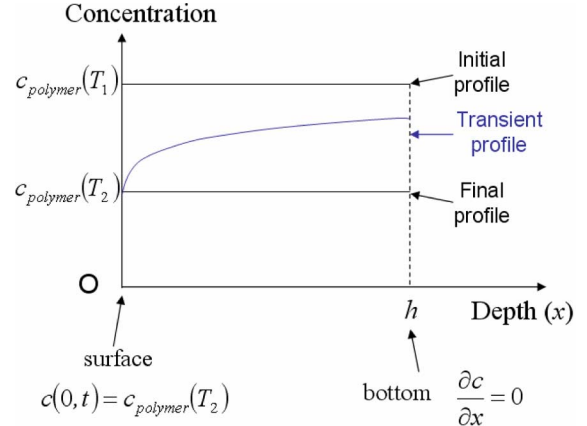


Fig. 1. Illustration of the diffusion problem when temperature increases instantaneously from  $T_1$  to  $T_2$ .

Solving (3) under the conditions of (4a)–(4c) and using (1), we derive the following expression for the vapor molecule concentration profile in the polymer (the solution for the partial differential equation (3) is found in, e.g., [11]):

$$c(x,t) = c_{\text{vapor}} \left[ K(T_2) - \frac{4}{\pi} (K(T_2) - K(T_1)) \cdot \sum_{m=1}^{\infty} \left[ \frac{1}{2m-1} \exp\left(-\frac{\pi(2m-1)^2 D_{T_2} t}{4h^2}\right) \times \sin\left(\frac{\pi}{2h}(2m-1)x\right) \right] \right]. \quad (5)$$

The change in local conductivity is assumed linearly proportional to the local vapor concentration, hence

$$\Delta\sigma(x) = -Nc(x) \quad (6)$$

where  $N$  is a constant. To calculate the fractional difference of the transient conductance  $G$  of a thin-film sensor, it is necessary to integrate the local conductance change along a line orthogonal to the film plane. (Note: This assumes that the electric field is a constant within the field and so independent of distance  $x$ ; and is a reasonable approximation when the interdigitated electrode gap is larger than the film thickness. Otherwise, the electric field is nonlinear and the line integral has a geometric term.):

$$\begin{aligned} \frac{\Delta G(t)}{G_{T_2, \text{dry}}} &= \frac{G_{T_2}(t) - G_{T_2, \text{dry}}}{G_{T_2, \text{dry}}} = \frac{1}{h} \int_0^h \Delta\sigma(x) dx \\ &= -Nc_{\text{vapor}} \left[ K(T_2) - \frac{8}{\pi^2} \cdot \{K(T_2) - K(T_1)\} \cdot \sum_{m=1}^{\infty} \left[ \frac{1}{2m-1} \exp\left(-\frac{\pi(2m-1)^2 D_{T_2} t}{4h^2}\right) \right] \right] \end{aligned} \quad (7)$$

where  $G_{T_2, \text{dry}}$  is the conductance in dry air (without any vapors). Using the following well-known formula to calculate the infinite series (see [12])

$$\sum_{k=1}^{\infty} \frac{1}{(2k-1)^2} = \frac{\pi^2}{8} \quad (8)$$

we find the initial and final values of the fractional change in conductance as follows:

$$\frac{\Delta G(0)}{G_{T2,dry}} = -Nc_{vapor}K(T_1) \quad (9a)$$

$$\frac{\Delta G(\infty)}{G_{T2,dry}} = -Nc_{vapor}K(T_2). \quad (9b)$$

These parameters are proportional to both vapor concentration and partition coefficient at the two temperatures. Using (7), (9a), and (9b), the amplitude and the normalized transient of (7) is calculated as follows:

(Amplitude)

$$\left| \frac{\Delta G(\infty)}{G_{T2,dry}} - \frac{\Delta G(0)}{G_{T2,dry}} \right| = N[K(T_1) - K(T_2)]c_{vapor} \quad (10a)$$

(Normalized transient)

$$\begin{aligned} & \left[ \frac{\Delta G(t)}{G_{T2,dry}} - \frac{\Delta G(0)}{G_{T2,dry}} \right] / \left[ \frac{\Delta G(\infty)}{G_{T2,dry}} - \frac{\Delta G(0)}{G_{T2,dry}} \right] \\ &= 1 - \frac{8}{\pi^2} \sum_{m=1}^{\infty} \left[ \frac{1}{2m-1} \exp\left(-\frac{\pi(2m-1)^2 D_{T2} t}{4h^2}\right) \right]. \end{aligned} \quad (10b)$$

The other transient (temperature decreased from  $T_2$  to  $T_1$ ) is found the same way and thus the results are written as follows. (Note: Here the diffusion coefficient is  $D_{T1}$  rather than  $D_{T2}$  as the diffusion is assumed to take place at  $T_1$  this time.)

(Concentration profile)

$$\begin{aligned} c(x,t) &= c_{vapor} \left[ K(T_1) - \frac{4}{\pi}(K(T_1) - K(T_2)) \cdot \right. \\ & \left. \sum_{m=1}^{\infty} \left[ \frac{1}{2m-1} \exp\left(-\frac{\pi(2m-1)^2 D_{T1} t}{4h^2}\right) \right] \right. \\ & \left. \times \sin\left(\frac{\pi}{2h}(2m-1)x\right) \right] \quad (11) \end{aligned}$$

(Fractional difference of the transient conductance)

$$\begin{aligned} \frac{\Delta G(t)}{G_{T1,dry}} &= \frac{G_{T1}(t) - G_{T1,dry}}{G_{T1,dry}} \\ &= -Nc_{vapor} \left[ K(T_1) - \frac{8}{\pi^2} \{K(T_1) - K(T_2)\} \cdot \right. \\ & \left. \sum_{m=1}^{\infty} \left[ \frac{1}{2m-1} \exp\left(-\frac{\pi(2m-1)^2 D_{T1} t}{4h^2}\right) \right] \right] \quad (12) \end{aligned}$$

(Amplitude of the fractional difference of the transient conductance)

$$\left| \frac{\Delta G(\infty)}{G_{T1,dry}} - \frac{\Delta G(0)}{G_{T1,dry}} \right| = N[K(T_1) - K(T_2)]c_{vapor} \quad (13a)$$

(Normalized fractional difference of the transient conductance)

$$\begin{aligned} & \left[ \frac{\Delta G(t)}{G_{T1,dry}} - \frac{\Delta G(\infty)}{G_{T1,dry}} \right] / \left[ \frac{\Delta G(\infty)}{G_{T1,dry}} - \frac{\Delta G(0)}{G_{T1,dry}} \right] \\ &= \frac{8}{\pi^2} \sum_{m=1}^{\infty} \left[ \frac{1}{2m-1} \exp\left(-\frac{\pi(2m-1)^2 D_{T1} t}{4h^2}\right) \right]. \end{aligned} \quad (13b)$$

From (10a) and (10b) (or (13a) and (13b)), we can conclude the following.

- The amplitude of the fractional difference of transient conduction is proportional to the ambient vapor concentration (proportionality constant is given by  $N[K(T_1) - K(T_2)]$ ).
- The shape of the normalized fractional difference of transient conductance curve depends on the diffusion coefficient, which is vapor-specific, but independent of the ambient vapor concentration.

Therefore, it should be possible to identify different vapors with just one chemical sensor using the shape of the curve and then quantify them using the amplitude.

It should be noted that we have considered an ideal situation, i.e., the thermal response time of the microhotplate is negligible, and thus we have used the time-independent conductance in dry air  $G_{T2,dry}$  to calculate the fraction for (7) and (12). However, in practice, the response time of the electrical conductance of polymer has a finite value (e.g., 10 ms) even in dry air, and thus the following expression with time dependent conductance in dry air should be used to preprocess the experimental data rather than (7) and (12):

$$\frac{\Delta G(t)}{G_{T2,dry}(t)} = \frac{G_{T2}(t) - G_{T2,dry}(t)}{G_{T2,dry}(t)}. \quad (14)$$

Therefore, we require the transient conductance of both with and without vapors to determine (14).

Finally, concentration profiles of (5) and (11) for  $h = 1 [\mu\text{m}]$  and  $D_{T1} = D_{T2} = 1 \times 10^{-8} [\text{cm}^2/\text{s}]$  is calculated and plotted in Fig. 2. Also, a normalized fractional difference of transient conductance when the temperature increases from  $T_1$  to  $T_2$  for  $h = 1 [\mu\text{m}]$  and  $D_{T2} = 1 \times 10^{-7}, 1 \times 10^{-8}, 1 \times 10^{-9} [\text{cm}^2/\text{s}]$  is calculated and plotted in Fig. 3.

### III. MODELING OF TRANSIENT CONDUCTANCE ASSOCIATED WITH A TEMPERATURE STEP IN A MIXTURE OF VAPORS

In this section, the transient conductance of the carbon black/polymer composite, associated with a temperature step in a mixture of  $n(\geq 2)$  vapors, is discussed. Again, we first consider the transient when the temperature steps up from  $T_1$  to  $T_2$  (i.e., when  $T_1 < T_2$ ). Assuming that the diffusion coefficient of one vapor molecule species is not affected by other vapor species (Note: This assumption should be correct as long as the concentrations of vapors in the polymer are low enough. Thus, it is required to choose the type of polymer and temperatures  $T_1$  and  $T_2$  carefully.), the diffusion equation for each vapor can be solved independently and in exactly the same way as described in the previous section. Thus, the transient concentration profile of each vapor may be written as follows:

$$\begin{aligned} c_i(x,t) &= c_{vapor,i} \left[ K_i(T_2) - \frac{4}{\pi}(K_i(T_2) - K_i(T_1)) \cdot \right. \\ & \left. \sum_{m=1}^{\infty} \left[ \frac{1}{2m-1} \exp\left(-\frac{\pi(2m-1)^2 D_{T2,i} t}{4h^2}\right) \right] \right. \\ & \left. \times \sin\left(\frac{\pi}{2h}(2m-1)x\right) \right] \quad (15) \end{aligned}$$

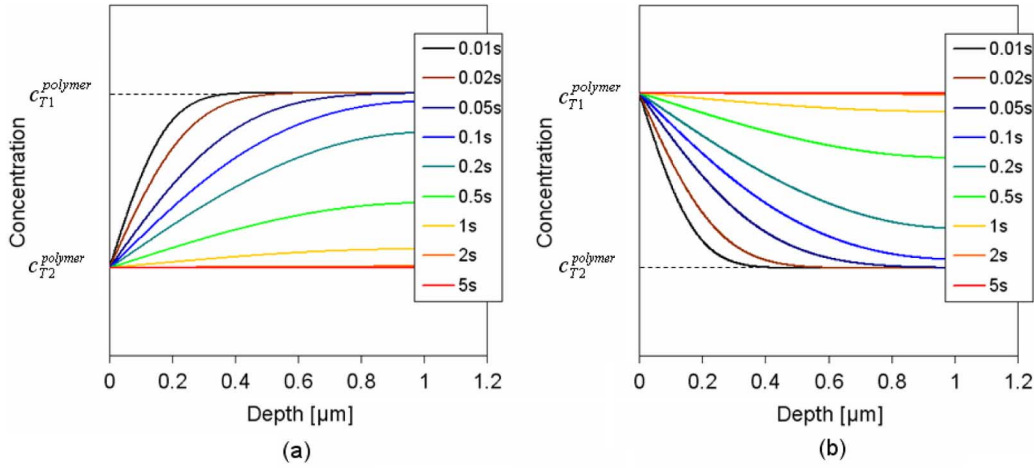


Fig. 2. Calculated transient concentration profiles (a) when temperature step increases from  $T_1$  to  $T_2$  and (b) when temperature step decreases from  $T_2$  to  $T_1$ .

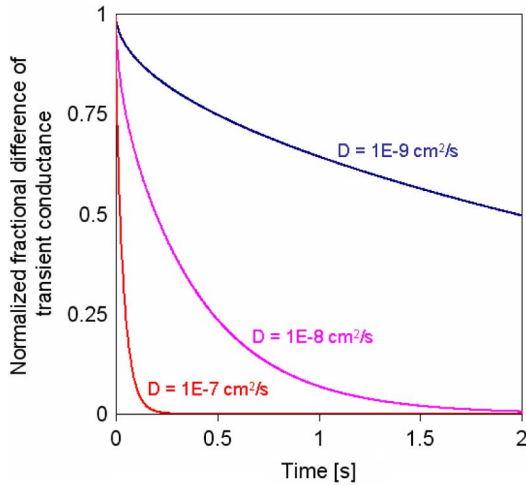


Fig. 3. Calculated normalized fractional difference of transient conductance when temperature steps up from  $T_1$  to  $T_2$ .

where the subscript  $i$  denotes the vapor species. Previous work has shown that the response of carbon/black polymer composite is generally linearly additive for organic vapors [13]. Therefore, it is natural to assume that the change in local conductivity is proportional to the weighted sum of the local concentration of all the vapors in the mixtures

$$\Delta\sigma(x) = - \sum_{i=1}^n N_i c_i(x) \quad (16)$$

where  $N_i$  is the proportional constant that is specific to the type of vapors. Thus, the fractional response is

$$\begin{aligned} \frac{\Delta G(t)}{G_{T2,dry}(t)} &= \frac{G_{T2}(t) - G_{T2,dry}(t)}{G_{T2,dry}(t)} = \frac{1}{h} \int_0^h \Delta\sigma(x) dx \\ &= \sum_{i=1}^n N_i c_{vapor,i} \left[ K_i(T_2) - \frac{8}{\pi^2} \{ K_i(T_2) - K_i(T_1) \} \cdot \right. \\ &\quad \left. \sum_{m=1}^{\infty} \left[ \frac{1}{2m-1} \exp\left(-\frac{\pi(2m-1)^2 D_{T2,i} t}{4h^2}\right) \right] \right]. \quad (17) \end{aligned}$$

This is in effect the superposition of the transient for each vapor. Using (8) again we find following expressions:

$$\frac{\Delta G(0)}{G_{T2,dry}} = \sum_{i=1}^n N_i K_i(T_1) \cdot c_{vapor,i} \quad (18a)$$

$$\frac{\Delta G(\infty)}{G_{T2,dry}} = \sum_{i=1}^n N_i K_i(T_2) \cdot c_{vapor,i} \quad (18b)$$

(Amplitude)

$$\begin{aligned} A &= \left| \frac{\Delta G(\infty)}{G_{T2,dry}} - \frac{\Delta G(0)}{G_{T2,dry}} \right| \\ &= \sum_{i=1}^n N_i [K_i(T_1) - K_i(T_2)] \cdot c_{vapor,i} \\ &\equiv \sum_{i=1}^n a_i \cdot c_{vapor,i} \quad (19a) \end{aligned}$$

(Normalized transient)

$$\begin{aligned} &\left[ \frac{\Delta G(t)}{G_{T2,dry}} - \frac{\Delta G(\infty)}{G_{T2,dry}} \right] / \left[ \frac{\Delta G(0)}{G_{T2,dry}} - \frac{\Delta G(\infty)}{G_{T2,dry}} \right] \\ &= \sum_{i=1}^n \left[ 1 - a_i c_{vapor,i} / \sum_{i=1}^n a_i c_{vapor,i} \right. \\ &\quad \left. \cdot \frac{8}{\pi^2} \sum_{m=1}^{\infty} \left[ \frac{1}{2m-1} \exp\left(-\frac{\pi(2m-1)^2 D_{T2} t}{4h^2}\right) \right] \right] \\ &= \sum_{i=1}^n [1 - a_i c_{vapor,i} / A \cdot f_i(t)]. \quad (19b) \end{aligned}$$

The other transient (when temperature steps down from  $T_2$  to  $T_1$ ) is modeled in a similar way and the results can be written as follows:

(Concentration profile)

$$\begin{aligned} c_i(x, t) &= c_{vapor,i} \left[ K_i(T_1) - \frac{4}{\pi} (K_i(T_1) - K_i(T_2)) \right. \\ &\quad \left. \cdot \sum_{m=1}^{\infty} \left[ \frac{1}{2m-1} \exp\left(-\frac{\pi(2m-1)^2 D_{T1,i} t}{4h^2}\right) \right] \right. \\ &\quad \left. \times \sin\left(\frac{\pi}{2h} (2m-1)x\right) \right] \quad (20) \end{aligned}$$

(Fractional difference of the transient conductance)

$$\begin{aligned} \frac{\Delta G(t)}{G_{T1,dry}} &= \frac{G_{T1}(t) - G_{T1,dry}}{G_{T1,dry}} \\ &= \sum_{i=1}^n N_i c_{vapor,i} \left[ K_i(T_1) - \frac{8}{\pi^2} \{K_i(T_1) - K_i(T_2)\} \right. \\ &\quad \cdot \left. \sum_{m=1}^{\infty} \left[ \frac{1}{2m-1} \exp\left(-\frac{\pi(2m-1)^2 D_{T1,i} t}{4h^2}\right) \right] \right] \quad (21) \end{aligned}$$

(Amplitude of the fractional difference of the transient conductance)

$$\begin{aligned} A &= \left| \frac{\Delta G(\infty)}{G_{T2,dry}} - \frac{\Delta G(0)}{G_{T2,dry}} \right| \\ &= \sum_{i=1}^n N_i [K_i(T_1) - K_i(T_2)] \cdot c_{vapor,i} \\ &\equiv \sum_{i=1}^n a_i \cdot c_{vapor,i} \quad (22a) \end{aligned}$$

(Normalized fractional difference of the transient conductance)

$$\begin{aligned} g(t) &= \left[ \frac{\Delta G(t)}{G_{T2,dry}} - \frac{\Delta G(0)}{G_{T2,dry}} \right] \bigg/ \left| \frac{\Delta G(\infty)}{G_{T2,dry}} - \frac{\Delta G(0)}{G_{T2,dry}} \right| \\ &= \sum_{i=1}^n \left[ a_i c_{vapor,i} \bigg/ \sum_{i=1}^n a_i c_{vapor,i} \right. \\ &\quad \cdot \left. \frac{8}{\pi^2} \sum_{m=1}^{\infty} \left[ \frac{1}{2m-1} \exp\left(-\frac{\pi(2m-1)^2 D_{T2,i} t}{4h^2}\right) \right] \right] \\ &\equiv \sum_{i=1}^n [a_i c_{vapor,i} / A \cdot f_i(t)]. \quad (22b) \end{aligned}$$

From (19a) and (19b) (or (22a) and (22b)), it can be concluded that:

- c) The amplitude of the fractional difference of transient conductance is a weighted sum of the all the ambient vapor concentrations, where the weight is  $a_i = N_i [K_i(T_1) - K_i(T_2)]$ .
- d) The shape of the normalized fractional difference of transient conductance curve is a weighted average of the normalized transient curve  $f_i(t)$  of the all the vapors, where the weight is  $a_i c_{vapor,i}$ .

From these conclusions, it is possible to identify and quantify each vapor in a mixture. Again, the transient when temperature steps up from  $T_1$  to  $T_2$  is considered first. Suppose a transient curve for a mixture with amplitude of  $A_{exp}$  and the normalized transient curve of  $(t_j, g_j) (j = 1, \dots, N)$  (interval:  $\Delta t$ ) is measured. We can find  $c_{vapor,i}$  using a least-squares fit, i.e., choosing  $c_{vapor,1}, \dots, c_{vapor,n}$  that minimizes the following sum of the squares:

$$\begin{aligned} \chi^2 &= \sum_{j=1}^N [g_j - g((j-1)\Delta t)]^2 \\ &= \sum_{j=1}^N \left[ g_j - \sum_{i=1}^n [a_i c_{vapor,i} / A_{exp} \cdot f_i((j-1)\Delta t)] \right]^2. \quad (23) \end{aligned}$$

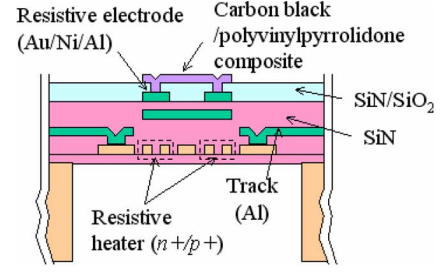


Fig. 4. Schematic cross section of a carbon black/PVP composite chemoresistor employing an SOI-CMOS based single crystal silicon microheater.

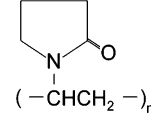


Fig. 5. Structural formula of PVP.

TABLE I  
LIST OF SENSORS USED

	Resistance [kΩ]	Thickness [μm]	Sheet resistance [kΩ]
PVP2	4.43	1.9	70.9
PVP8	1.91	6.0	30.6
PVP11	13.65	0.8	218.4

This is achieved by solving the following equations simultaneously:

$$\begin{cases} \frac{\partial \chi^2}{\partial c_{vapor,1}} = 0 \\ \vdots \\ \frac{\partial \chi^2}{\partial c_{vapor,n}} = 0 \end{cases}. \quad (24)$$

These equations can be solved generally as long as the following conditions are satisfied.

- I.  $a_i$  and  $f_i(t)$  are known.
- II. (Number of different vapors,  $n$ ) < (number of data points over time,  $N$ ).

Condition I can easily be achieved by premeasuring the transients for all the possible single vapors. Also, condition II is normally satisfied because the number of type of vapors ( $n$ ) is typically less than 10 and the number of data points over time ( $N$ ) is typically more than 10 (e.g., for transient time constant 1 s and interval time ( $\Delta t$ ) 10 ms,  $N$  is 1000). Therefore, it can be concluded that it is possible to identify and quantify each vapor in a mixture comprised of  $n$  ( $\geq 2$ ) types of vapors using this technique. [Note: Practically, it is not always easy to separate vapors in a mixture, especially when vapors do not have significantly different diffusion coefficients, as shown later. This is because all the transient curves of the single vapors are monotonously increasing (or decreasing).]

#### IV. DEPOSITION OF CARBON BLACK/POLYMER COMPOSITE MATERIALS ONTO MICROHOTPLATES

Fig. 4 shows a schematic cross section of the chemoresistor used in this work. The CMOS microhotplate comprises a sil-

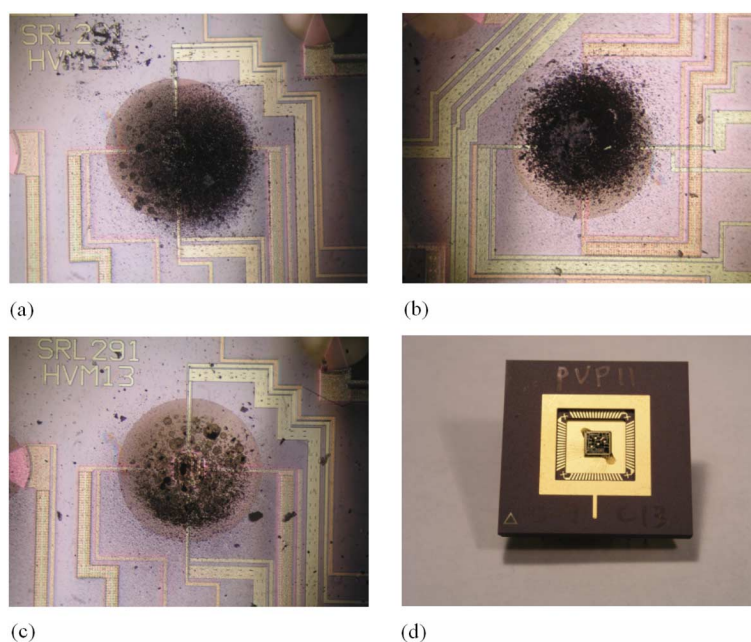


Fig. 6. Photographs of the SOI microhotplates with carbon black/PVP composite films. (a) PVP2, (b) PVP8, (c) PVP11, and (d) PVP11 bonded on 68 pin ceramic package.

icon nitride/silicon dioxide membrane in which a highly doped single crystal silicon (SCS) resistive heater is sandwiched. The shapes of both membrane and heater were designed to be circular to reduce the possibility of membrane failure due to mechanical stress at the edges. The radii of the membrane and the heater are 282 and 75  $\mu\text{m}$ , respectively. To supply the power to the micro-heaters, metal tracks were used to reduce both the Joule heat generated and the conductive heat loss. A second CMOS aluminium layer is used to form heat-spreading plates to improve the temperature uniformity of the sensing material (placed above the heaters). The electrodes used to measure the resistance of the sensing materials are made of the third CMOS aluminium layer onto which Au/Ni were electrodelessly plated (i.e., bump bonded) to make good, stable ohmic contact to the sensing material. These electrodes have interdigitated structures with an aspect ratios of 16. The microhotplate is described in more detail in [14].

Carbon black/polyvinylpyrrolidone (PVP) composite (20 wt % carbon black) was chosen as the sensing material. PVP in powder form was used with a molecular weight of *ca.* 40 000, supplied by Sigma Aldrich (U.K.). The structural formula of PVP is shown in Fig. 5. The polymer contains two atoms with strong electronegativity, i.e., oxygen and nitrogen (electronegativity of oxygen and nitrogen atoms are 3.5 and 3.0 in Pauling's definition) [15]. Therefore, it is expected that the carbon black/PVP composite has a larger sensitivity to polar vapors, such as alcohols, than nonpolar vapors. The carbon black nanospheres with a diameter of typically 50–80 nm (Black Pearls 2000) were supplied by Cabot Corporation (USA). The PVP was dissolved in pure ethanol at 50  $^{\circ}\text{C}$  using a magnetic stirrer for 12 h. Then, 0.3 g of carbon black was added and mixed with 20 ml of ethanol using a flask shaker (Griffin and George, U.K.) for 10 min. The mixture was deposited onto a microhotplate using a commercial air brush (HB-BC or HP-CP Iwata, Japan) through a mask made by microstereolithography. The device was bonded on a 68 pin ceramic package prior to

deposition, and the resistance of the film was measured during deposition in order to control the thickness. The mask has two circular holes, both of which had a diameter of 400  $\mu\text{m}$ , and the distance between their centers is 1.0 mm. One circular hole defined the area of the sensing film on the devices, and the other was used to measure the thickness of the film. After deposition, heat treatment at 50 $^{\circ}\text{C}$  for 24 h was carried out in an oven to evaporate the solvent and stabilize the sensor resistances. Finally, the sensors were exposed to the flow of dry air at 25  $^{\circ}\text{C}$  for 12 h using an FIA (flow injection analysis) test station (described later).

Table I lists the resistances, thicknesses, and sheet resistances of the three devices used in these experiments and Fig. 6 shows their photographs. They are referred to as PVP2, PVP8, and PVP11. The resistances of the film were measured at 25  $^{\circ}\text{C}$  in the dry air environment in the FIA test station. The film thickness of PVP8 was found to be *ca.* 6  $\mu\text{m}$  using an optical interferometer (Wyko/NT2000). The thicknesses of PVP2 and PVP11 were difficult to measure because they were comparable with the measurement noise (typically, 2 to 3  $\mu\text{m}$ ) caused by surface roughness (the value of which could be 2 to 3  $\mu\text{m}$  at the maximum). Therefore, it was decided to estimate the thickness of PVP11, which was deposited from the same solution on the same day as PVP8, by assuming that the resistance of the film is inversely proportional to the resistance. The thickness of PVP2 was also estimated using the same assumption. However, PVP2 is not used in this paper when discussing the thickness dependence, because it was deposited from a different solution synthesized on a different date.

The deposition technique using the airbrush is basic and manual. Therefore the repeatability strongly depends on the skill of the person who carries out the deposition. It is believed that the repeatability as well as the quality of the film (e.g., surface flatness and uniformity) would be improved by using a fully automated nanoliter noncontact dispensing system (e.g., [16]).

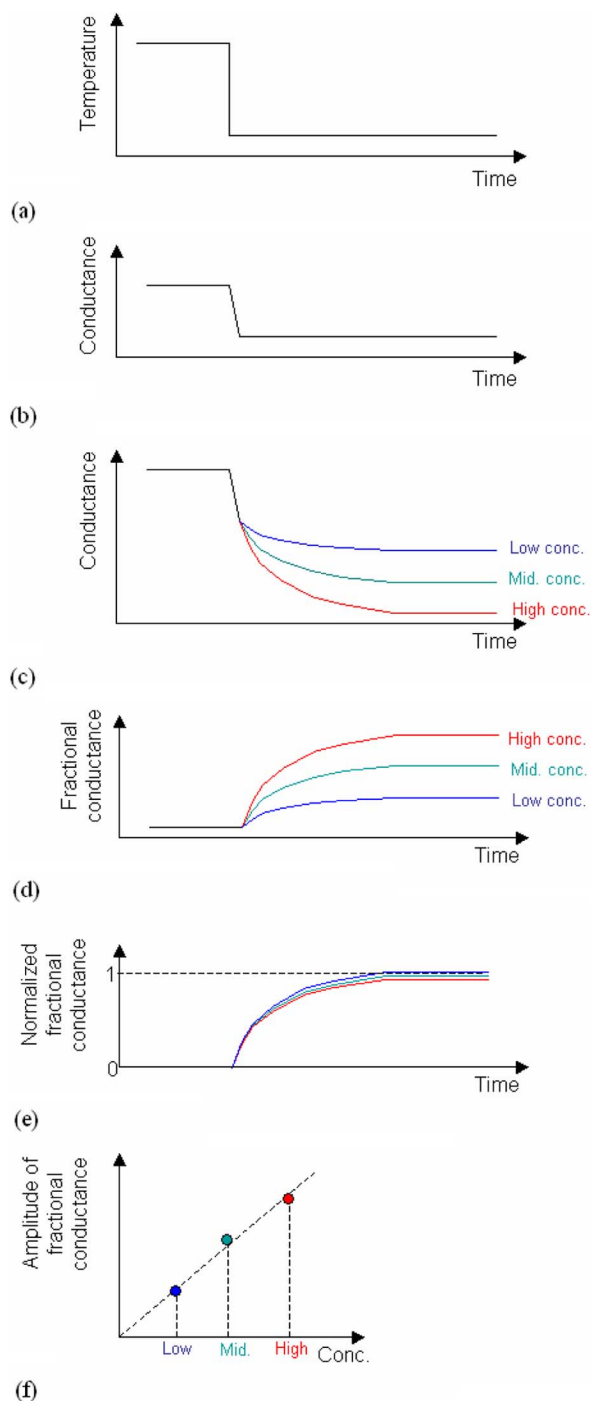


Fig. 7. Conceptual illustration of the proposed technique. (a) Temperature off transient. (b) Off transient of the sensor conductance in dry air (without vapors). (c) Off transient of sensor conductance in vapors of three different concentrations. (d) Fractional conductance in vapors. (e) Normalized fractional conductance in vapors. (f) Amplitude of fractional conductance.

## V. PROCESSING EXPERIMENTAL DATA

Before discussing the experimental results, the method of applying the proposed technique to the experimental data is explained, conceptually using Fig. 7, as follows.

- The temperature is switched between two temperatures using the CMOS microhotplate heater. Here, only the off-transient is considered for simplicity.

- The transient conductance signal of the carbon black/PVP composite film in dry air is first collected. The conductance changes (with relatively small time constant) even in dry air, since carbon black/polymer composite generally have finite temperature coefficients of resistances. (Here, the temperature coefficient of the resistance of the carbon black/PVP composite film is assumed to be negative. This turns out to be true for all the films studied in this paper, as shown later [17].)
- Then, the transient conductance signals of the sensors is recorded in different vapors. Note, the larger the vapor concentration, the larger the amplitude and time constant of the conductance change.
- Then, the fraction is calculated using the signals in Fig. 7(b) and (c), in order to cancel out the effect of the temperature dependence of the resistance.
- The transient curves are normalized. The shape of the resultant curve should be independent of the concentration, but depend on the analyte. Therefore, the time constant (for example, the time to reach 50% of the final value) is specific to the types of vapors and can be used for vapor identification.
- The amplitude of the fractional conductance curve [Fig. 7(d)] should be linearly proportional to the vapor concentration and used for quantification.

## VI. CHARACTERIZATION

Temperature modulation experiments of the three devices (PVP2, PVP8, and PVP11) were performed. The devices were glued and wire-bonded onto ceramic packages and mounted in a stainless steel chamber with the controlled temperature of 25°C in a fully automated FIA test station. The temperature of the carbon black/PVP composite film was controlled by applying a voltage to the microhotplate. The temperatures used in the experiments were 25 °C, 35 °C, 45 °C, and 55 °C, which require operating voltages (and powers) of 0 V (0 mW), 0.78 V (0.8 mW), 1.10 V (1.6 mW), and 1.35 V (2.4 mW), respectively. The accuracy of the temperature modulation amplitude was about  $\pm 0.3$  °C. The concentrations of water, methanol and ethanol vapors in the chamber were controlled independently with the uncertainty of only 5%. A constant current of 10  $\mu$ A was applied to the carbon black/PVP composite film and the voltage was recorded every 10 ms.

The results are discussed in the following order: (a) demonstration of the processing procedure, (b) concentration and vapor type dependence, (c) thickness dependence, (d) temperature dependence, and (e) mixture effect.

### A. Demonstration of the Processing Procedure

First of all, the concentration dependence of water vapor was studied using its “temperature off” transient to demonstrate the procedure of Fig. 7. Temperature modulation experiments of the device PVP2 were carried out with the presence of water vapor of different concentrations (0, 1000, 2000, 3000, 4500, 6000 ppm). The amplitude and frequency of the applied square wave voltage were 0.78 V (i.e., temperature modulation between 25 °C and 35 °C) and 50 mHz.

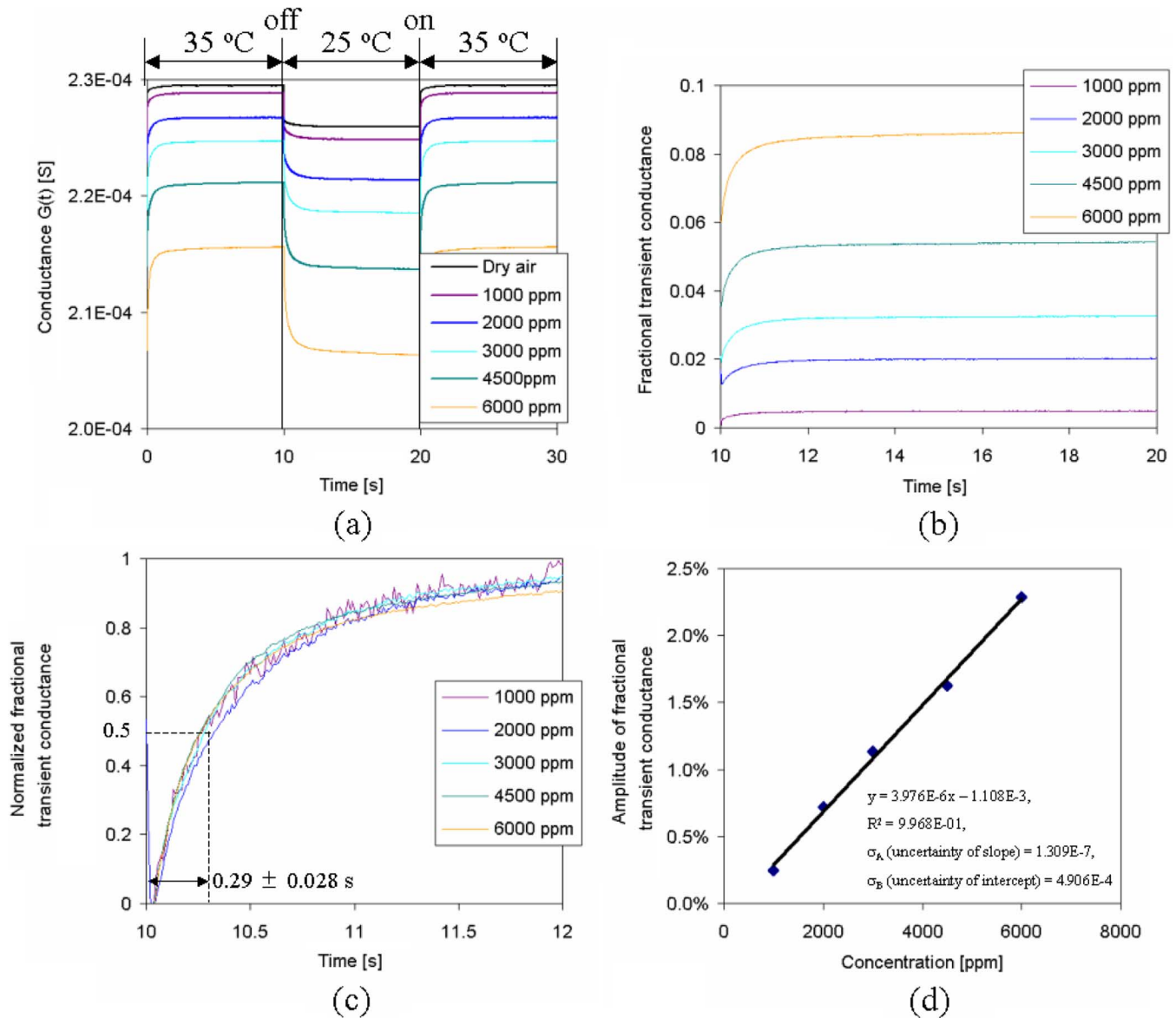


Fig. 8. Demonstration of the processing data using the experimental results of PVP2 in water vapor. (a) Raw data. (b) Fractional transient conductance. (c) Normalized fractional transient conductance. (d) Amplitudes of fractional transient conductance.

Fig. 8(a) shows the results. Each curve in Fig. 8(a) is the average of 30 transients. The temperature was 35 °C from 0 to 10 s and 20 to 30 s, and 25 °C from 10 to 20 s. (The conductance in dry air shows lower conductance at 25 °C, indicating the temperature coefficient of resistance is negative.) Then, by calculating the fraction using the curves from 10 to 20 s (temperature off transient) with and without vapor, we obtain Fig. 8(b). Finally, the normalized fractional conductance curves and the amplitude of the fractional conductance curves are plotted, as shown in Fig. 8(c) and (d). It was found that the shape of the normalized curves does not depend on vapor concentration and the amplitude of the fractional transient conductance curves is linearly proportional to the concentration, both as expected.

### B. Concentration and Vapor Type Dependence

Here, the results of temperature modulation experiments of device PVP2 are discussed. The experiments were performed in

the presence of water, methanol and ethanol vapors of different concentrations (water: 0, 1000, 2000, 3000, 4500, 6000 ppm, methanol: 1360, 2710, 4070, 5430 ppm, ethanol: 2270, 4540, 6810, 9080 ppm). The amplitude of the applied square wave voltage was 0.78 V (i.e., temperature modulation between 25 °C and 35 °C), and the frequency 50.0 mHz for water and methanol and 1.7 mHz for ethanol (lower frequency was used for ethanol due to its smaller diffusion coefficient in PVP compared to water and methanol).

Figs. 9–11 are the normalized fractional transient conductance curves of the (a) off and (b) on-transients in water, methanol and ethanol vapors. The curves for water and methanol are averages of 30 transients and that for ethanol is an average of 3 transients. (For ethanol, the data taken every 10 ms were averaged and plotted every 0.3 s for noise reduction). The results indicate that the shape of the normalized fractional transient conductance curves are independent of vapor concentration but depend on vapor type, as predicted.



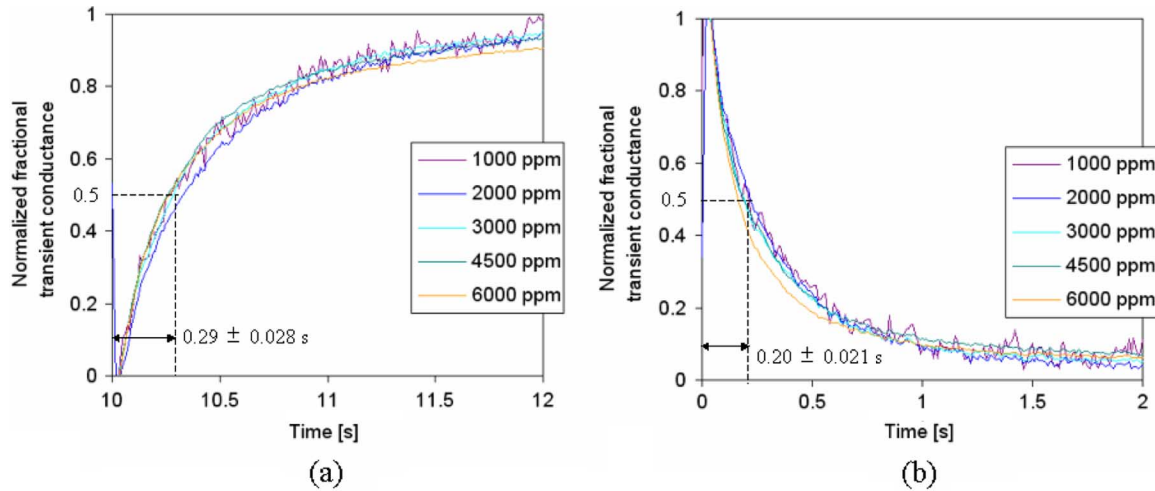


Fig. 9. Normalized fractional transient conductance of PVP2 in water vapor at different concentrations: (a) off transient and (b) on transient.

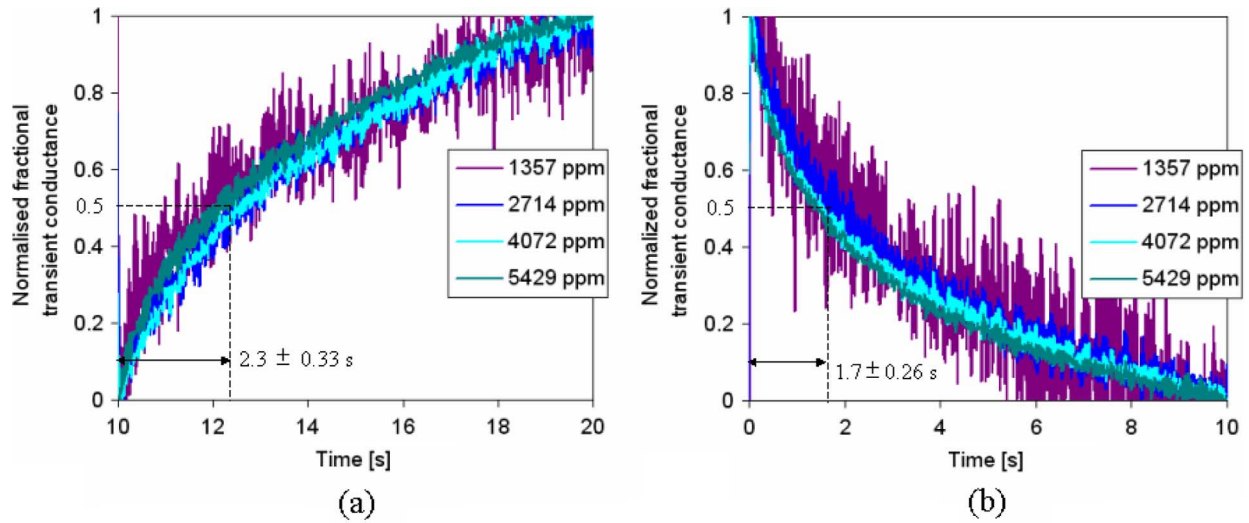


Fig. 10. Normalized fractional transient conductance of PVP2 in methanol vapor at different concentrations: (a) off transient and (b) on transient.

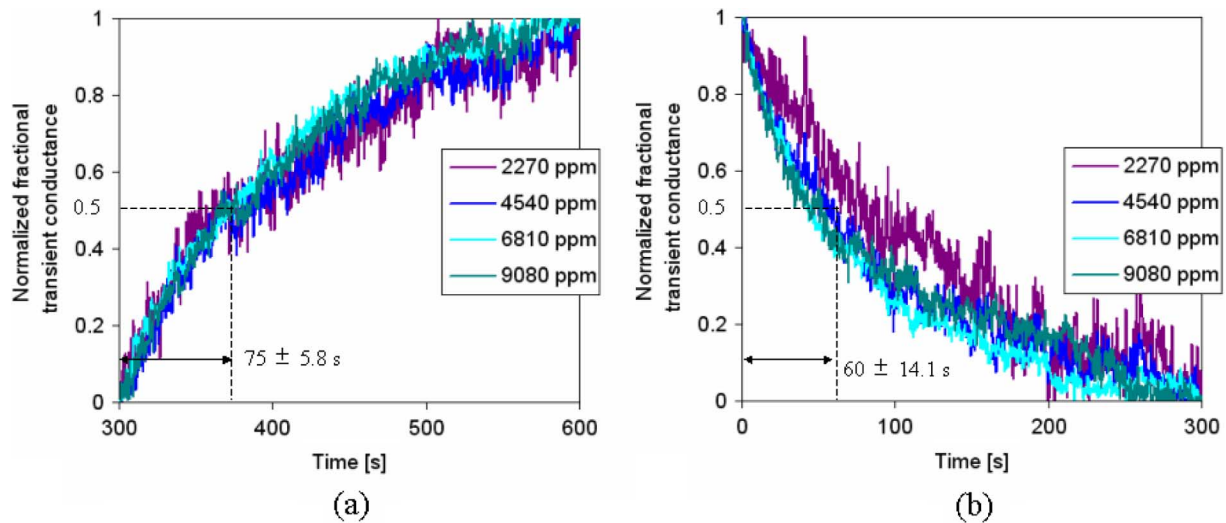


Fig. 11. Normalized fractional transient conductance of PVP2 in ethanol vapor at different concentrations: (a) off transient and (b) on transient.

Table II lists the time constants of the normalized fractional transient conductance curves. The time constant of water is the

smallest and that of ethanol the largest. Considering that the molecular mass of water is the smallest and that of ethanol is

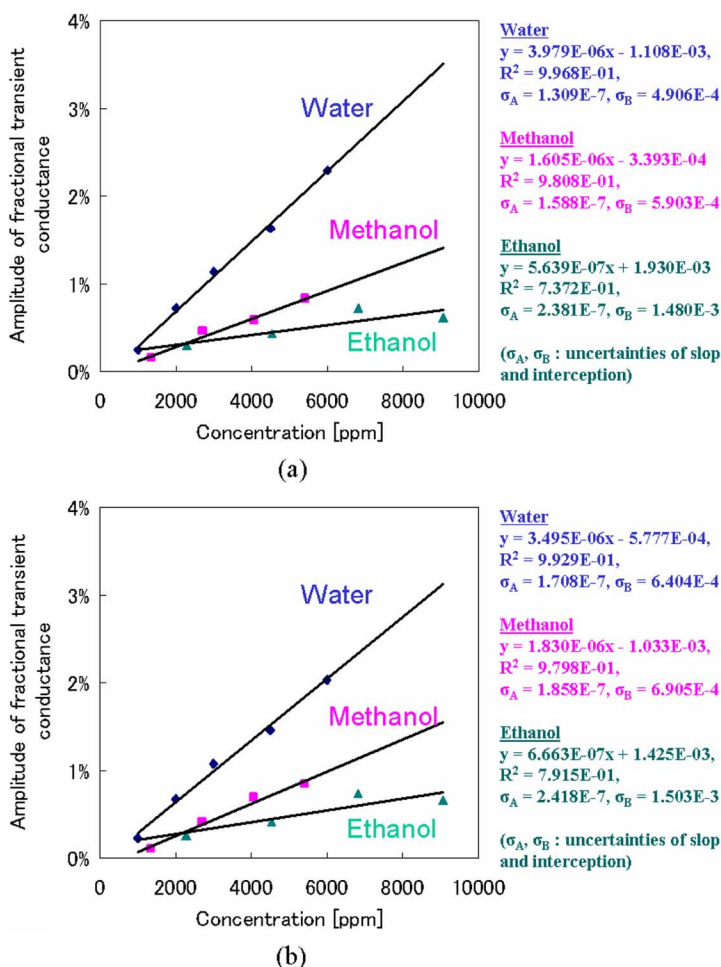


Fig. 12. Amplitudes of fractional transient conductance of PVP2 in water, methanol, and ethanol vapors: (a) off transient and (b) on transient.

TABLE II  
 TIME CONSTANTS ( $t_{50\%}$ ) OF NORMALIZED FRACTIONAL TRANSIENT CONDUCTANCE CURVES OF PVP2 IN WATER, METHANOL, AND ETHANOL VAPOR

	water	methanol	ethanol
off transient	0.29 s ± 0.028 s	2.3 s ± 0.33 s	75 s ± 5.8 s
on transient	0.20 s ± 0.021 s	1.7 s ± 0.26 s	60 s ± 14.1 s

the largest, this result indicates that the species with low molecular mass diffuse faster (molecular mass of water, methanol and ethanol are 18, 32, and 46 [18]). The time constant of off-transient is smaller than that of on-transient for each vapor. This is reasonable, considering that the temperature of off-transient (25 °C) is lower than that of on-transient (35 °C) and the diffusion coefficient tends to be larger at higher temperatures.

Fig. 12 plots the amplitude of fractional transient conductance versus concentration of water, methanol and ethanol for both the (a) off and (b) on-transients. The amplitude of the fractional transient conductance curve of all water, methanol and ethanol for both the off- and on-transients is linearly proportional to the concentration, again, as predicted.

Finally, identification and quantification of vapors were carried out. The amplitude of the fractional transient conductance versus the time constant ( $t_{50\%}$ ) for the off and on-transients

were plotted, as shown in Fig. 13. The plots clearly show that identification and quantification of water, methanol, and ethanol vapors was successfully carried out using the proposed technique with either the off or on-transients of the temperature modulated signal.

C. Thickness Dependence

The thickness dependence was also investigated. For this experiment, devices PVP8 and PVP11 were used. Their thickness was *ca.* 6.0 μm and *ca.* 0.8 μm, respectively. The devices were tested to water with a concentration of 3000 ppm. The amplitude of the applied square wave voltage was 0.78 V (i.e., temperature modulation between 25 °C and 35 °C), and the frequency 50 mHz.

Fig. 14 shows the normalized transient fractional conductance of both (a) off and (b) on-transient. Each curve in Fig. 14 is the average of 30 transients. Table III lists the time constants ( $t_{50\%}$ ) of PVP8 and PVP11 for both off and on-transients. The time constant of the thicker film (PVP8) was 17.5 and 11.0 times as large as that of thinner film (PVP11) in off and on-transient, respectively. The results suggest it is possible to modify the time constant of the proposed technique by simply modifying the thickness of the sensing film. This will allow the detection of molecules with much smaller diffusion coefficients in a shorter

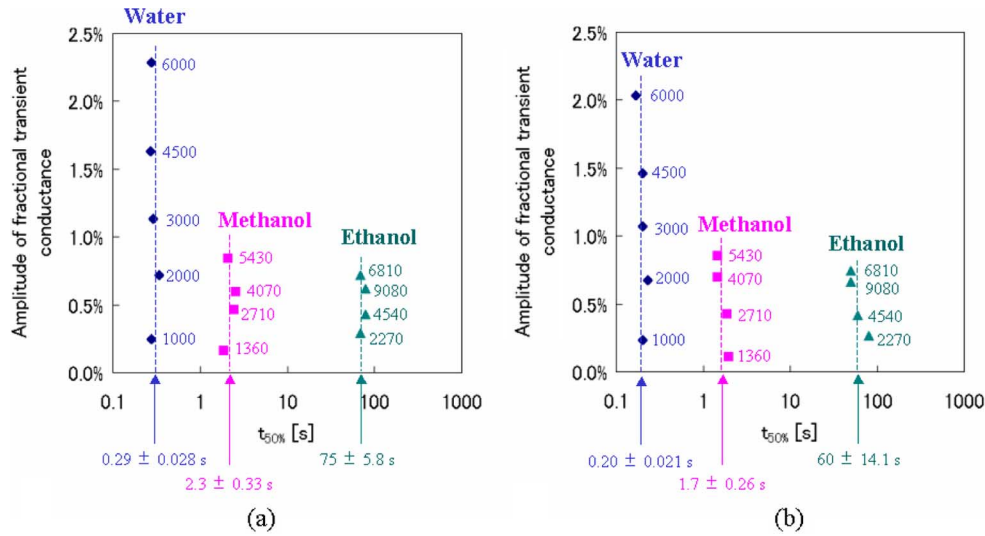


Fig. 13. Identification and quantification of water, methanol and ethanol vapor using (a) off transient and (b) on transient of conductance curves of PVP2.

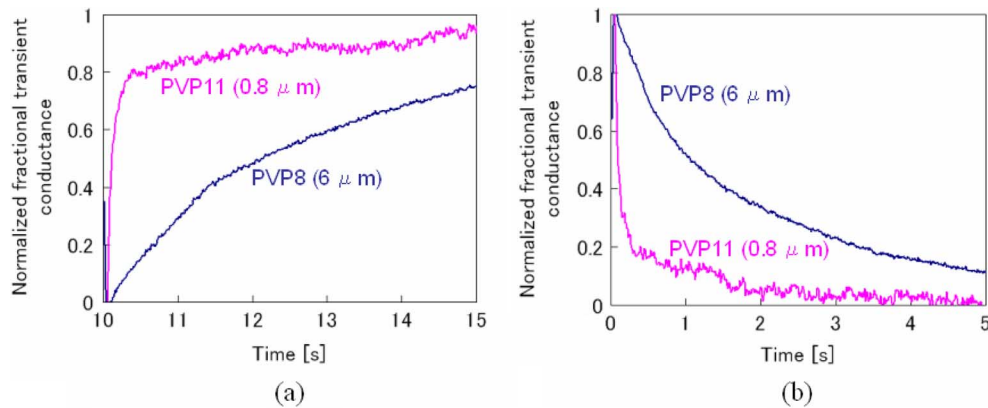


Fig. 14. Normalized fractional transient conductance of PVP8 and PVP11 at 3000 ppm water vapor: (a) off transient and (b) on transient.

TABLE III  
TIME CONSTANTS ( $t_{50\%}$ ) OF NORMALIZED FRACTIONAL TRANSIENT CONDUCTANCE CURVES OF PVP8 AND PVP11 AT 3000 ppm WATER VAPOR

	PVP8 (6.0 $\mu\text{m}$ )	PVP11 (0.8 $\mu\text{m}$ )
off transient	2.1 s	0.12 s
on transient	1.1 s	0.10 s

period of time. The theory described previously predicts that the time constant should be proportional to the square of the thickness. Therefore, the time constant of the thicker film should be  $(6.0 \mu\text{m}/0.8 \mu\text{m})^2 = 56$  times as much as that of the thinner one, theoretically. The discrepancy between the experiments and the theory is probably reasonable considering the uncertainty in deposition and thickness measurements and the variation in thickness of the film across the sensor.

#### D. Temperature Dependence

The temperature dependence of the steady-state and transient state were investigated using methanol vapor with a concentration of 2710 ppm and the PVP11 sensor. (Measurements were also carried out in dry air for comparison). The

TABLE IV  
SATURATED CONDUCTANCE OF PVP11 WHEN THE TEMPERATURE WAS MODULATED BETWEEN 25 °C AND 35 °C WITH AND WITHOUT METHANOL VAPOR

	$G_{dry}$	$G_{methanol}$	$\Delta G/G_{dry}$
25 °C	7.412E-05	7.230E-05	2.46%
35 °C	7.538E-05	7.404E-05	1.78%

amplitude of the applied square wave voltage was 0.78, 1.10, and 1.35 V, which corresponds to temperature modulation of 25 °C  $\leftrightarrow$  35 °C, 25 °C  $\leftrightarrow$  45 °C and 25 °C  $\leftrightarrow$  55 °C, respectively. The frequency was 10 mHz (retention time: 50 s).

First of all, the steady-state conductance with and without methanol vapor was considered. The conductance values taken after 50 s (= retention time) from the off or on-transients are used as the saturated values (or steady-state values) and shown in Tables IV–VI. Fig. 15 shows the plot of logarithm of the steady-state response  $((G_{dry} - G_{methanol})/G_{dry})$  versus the inverse of the absolute temperature ( $1/T$ ). Their relation is linear, and

TABLE V  
SATURATED CONDUCTANCE OF PVP11 WHEN THE TEMPERATURE WAS MODULATED BETWEEN 25 °C AND 45 °C WITH AND WITHOUT METHANOL VAPOR

	$G_{dry}$	$G_{methanol}$	$\Delta G/G_{dry}$
25 °C	7.416E-05	7.230E-05	2.51%
45 °C	7.651E-05	7.555E-05	1.26%

TABLE VI  
SATURATED CONDUCTANCE OF PVP11 WHEN THE TEMPERATURE WAS MODULATED BETWEEN 25 °C AND 55 °C WITH AND WITHOUT METHANOL VAPOR

	$G_{dry}$	$G_{methanol}$	$\Delta G/G_{dry}$
25 °C	7.415E-05	7.232E-05	2.47%
55 °C	7.746E-05	7.677E-05	0.89%

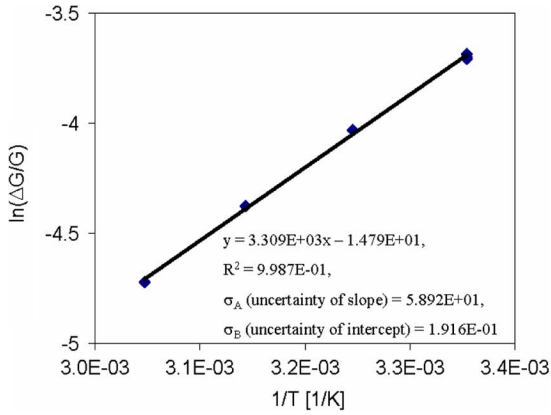


Fig. 15. Temperature dependence of steady-state response of PVP11 in methanol vapor.

this is expected as steady-state response is known to follow the following relationship:

$$\frac{\Delta G}{G_{dry}} = \frac{G_{dry} - G_{methanol}}{G_{dry}} \propto \exp\left(-\frac{\Delta H_0}{RT}\right) \quad (25)$$

where  $\Delta H_0$  is the standard enthalpy change for the interaction between the polymer and the vapor molecule and  $R$  the gas constant [19]. Therefore, it is possible to calculate the standard enthalpy from the slope of Fig. 15, and the value was found to be  $-27.5$  [kJ/mol]. The negative value indicates that the absorption is exothermic reaction, and the relatively small value ( $<30$  kJ) shows that the adsorption mechanism is physisorption rather than chemical reaction [19].

Then, the transient behavior was investigated. Fig. 16(a) and (b) are the normalized fractional transient conductance curves of the off and on-transient when the temperature modulated in the following ways: 25 °C  $\leftrightarrow$  35 °C, 25 °C  $\leftrightarrow$  45 °C, and 25 °C  $\leftrightarrow$  55 °C. The signals are the averages of the six transients. By subtracting the signals of Fig. 16(b) from the unity and plotting with those shown in Fig. 16(a), the curves in Fig. 16(c) are obtained. The figure shows that the response becomes faster as the

temperature increases, as predicted. Fig. 16(d) shows that the relationship between the logarithm of the response time ( $t_{50\%}$ ) and the inverse of the temperature ( $1/T$ ) is linear. Since the diffusion coefficient is inversely proportional to the time constant, it is apparent that the temperature dependence of the diffusion coefficient is Arrhenius type, with the activation energy ( $E_a$ ) of 0.40 eV, which was calculated by the following equation:

$$E_a = k_B \times (\text{slope}) \quad (26)$$

where  $k_B$  is the Boltzmann constant.

### E. Mixture

Finally, the response to a binary mixture was investigated. The device PVP2 was tested to a mixture of 2000 ppm water and 2710 ppm methanol in air. The amplitude and frequency of the applied square wave voltage was 0.78 V (i.e., temperature modulation between 25 °C and 35 °C) and frequency of 50 mHz.

Fig. 17(a) and (b) show the normalized transient fractional conductance of both the (a) off and (b) on-transient in the mixture. Each curve in Fig. 17 is the average of 30 transients. The results of single vapor of 2000 and 2710 ppm methanol and the predicted curves from the single vapor results are also plotted in the same figures. Table VII shows the amplitude of all the above curves (before normalization) including the prediction. It was found that the experimental curve in the mixture is close to that predicted.

The results indicate that the above technique could be employed to identify and quantify each vapor in a binary mixture. However, one caveat should be given. The technique uses monotonously increasing (or decreasing) curves only. This means it is needed to separate out several curves with different time constants from noisy experimental curves in order to deal with a mixture with several different vapors, a process that is not always easy.

## VII. CONCLUSION

In this paper, a novel temperature modulation technique for a single carbon black/polymer composite sensor has been proposed in order to enable it to discriminate between different vapors. The technique can be summarized as follows.

1. Apply a square wave voltage to a resistive microheater to step change the sensor temperature and measure the transient sensor conductance in the presence of different vapors.
2. Use the fractional difference in transient conductance as the preprocessing feature.
- 3a. For a single vapor, the amplitude of the fractional difference of transient conductance is used to predict the concentration; whilst the shape of the normalized curve (which is independent of vapor concentration but dependent upon vapor type) to predict vapor type.
- 3b. For a mixture of  $n$  ( $\geq 2$ ) components, fractional difference of transient conductance is predicted to be superposition of those of single vapors, i.e., the fractional difference of transient conductance of a mixture is the linear combination of

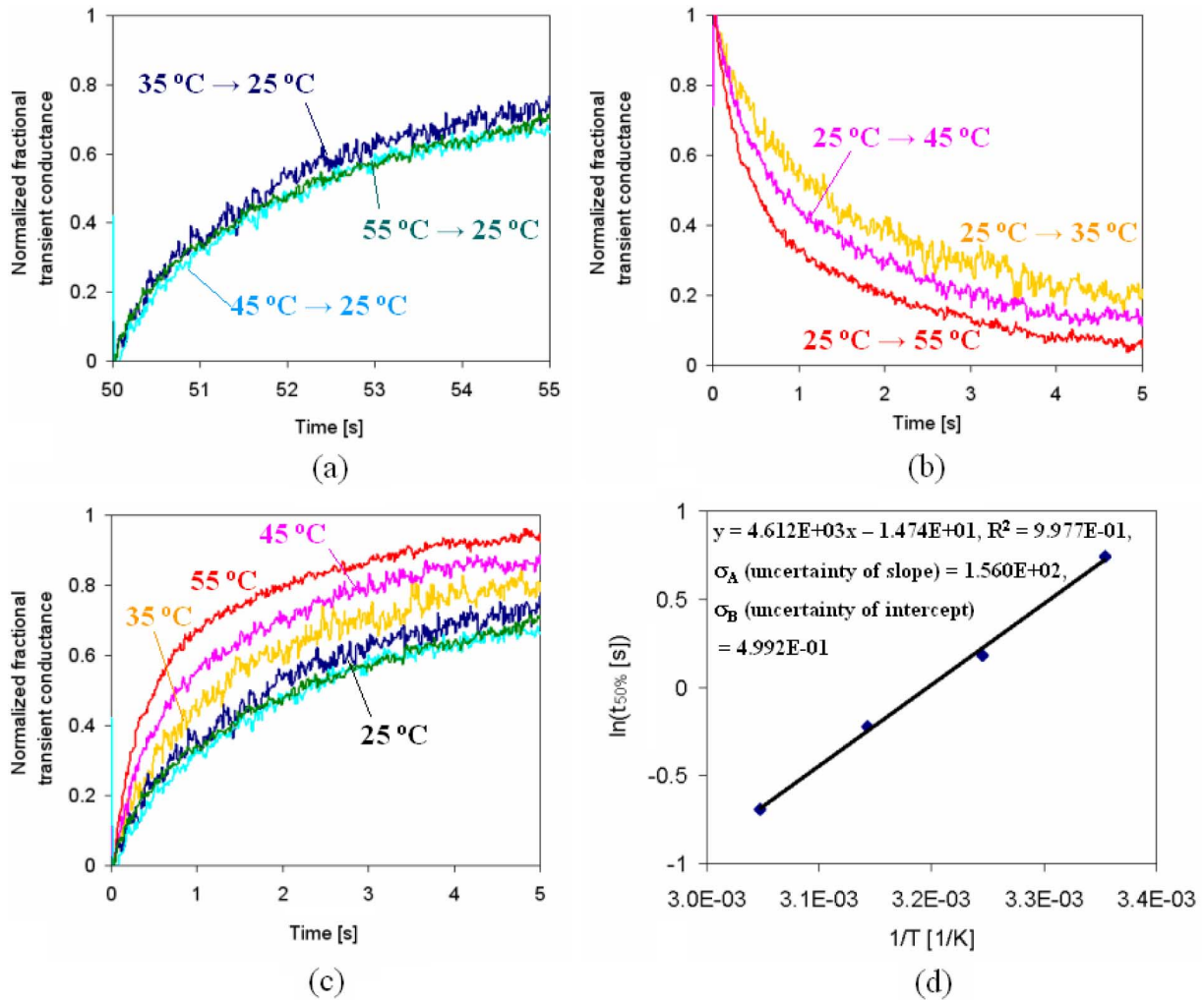


Fig. 16. Temperature dependence of the steady-state response of PVP11 in methanol vapor: (a) off transient, (b) on transient, (c) off and on transient, and (d) logarithm of time constant versus inverse of absolute temperature.

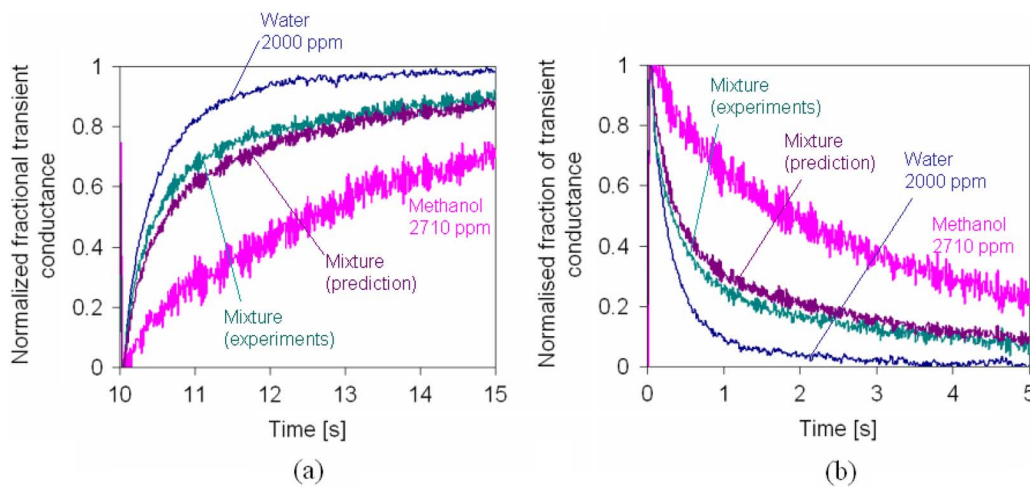


Fig. 17. Normalized fractional transient conductance of PVP2 in a mixture of 2000 ppm water and 2710 ppm methanol vapor: (a) off transient and (b) on transient.

that of each component with the coefficient being proportional to the concentration of each component, as shown in (22b). Those coefficients are found by applying the least squares method to an experimental curve [i.e., by solving

(24)]. Therefore, identification and quantification of each vapor in a mixture is possible, as long as the conditions I and II in Section III are satisfied and the signal to noise ratio is large enough.

TABLE VII  
AMPLITUDE OF FRACTIONAL TRANSIENT CONDUCTANCE OF PVP2 IN A SINGLE VAPOR OF WATER AND METHANOL, AND THE MIXTURE

Water 2000 ppm	Methanol 2710 ppm	Mixture (actual value)	Mixture (predicted value)
0.72 %	0.46 %	1.21 %	1.18 %

The proposed technique was applied to CMOS microhotplate-based carbon black/PVP chemoresistors. Identification and quantification of single vapors of water, methanol and ethanol with different concentrations (water: 0–6000 ppm, methanol: 1360–5430 ppm, ethanol: 2270–9080 ppm) were successfully demonstrated.

Next, the technique was applied to a mixture of water and methanol with the concentrations of 2000 and 2710 ppm, respectively. The results indicate that the transient curves of the mixture are the superposition of single vapors, though more experiments are needed to confirm this observation.

The device power needed to keep the temperature at 35 °C, 45 °C, and 55 °C continuously were 0.8, 1.6, and 2.4 mW, respectively. Since the temperature modulation was performed by applying a square wave voltage (produced by simply switching on and off the operating voltage of the heater) with a duty ratio of 50 %, the average operating power of the sensor is half of the DC values, i.e., 0.4, 0.8, and 1.2 mW for 35 °C, 45 °C, and 55 °C, respectively. The value is much lower than those of metal oxide-based chemoresistors. For example, Llobet *et al.* reported on results of multicomponent gas mixture analysis using Pd doped tin oxide film on a platinum based microhotplate [20]. They modulated the temperature between 243 °C and 405 °C by applying a sinusoidal wave voltage, and it requires much more than 80 mW (which is a value needed to operate their microhotplate at the minimum temperature of 243 °C continuously [21]). In addition, it should be noted that it is possible to reduce the power consumption by more than 50% by using the smaller SOI CMOS microhotplates developed by ourselves, as shown in [14].

Finally, two limitations of the proposed technique are pointed out. First of all, it is not always easy to identify the components of a mixture using a simple least squares method, since several monotonously increasing (or decreasing) curves with different time constants need to be separated out from noisy experimental curves. Second, the technique requires the signal in the dry air as the baseline. Since the baseline resistance is likely to change over time, it is necessary to calibrate the zero gas transient on a regular basis. An extended technique to obviate these two limitations is proposed elsewhere [22].

## REFERENCES

- [1] United States Environmental Protection Agency (EPA), "Indoor air facts No. 4 (Revised), sick building syndrome," 1991.
- [2] UK Air Quality Archive accessed on Nov. 15, 2007. [Online]. Available: <http://www.airquality.co.uk/archive/index.php>
- [3] C. M. Matzke, R. J. Kottenstette, S. A. Casalnuovo, G. C. Frye-Mason, M. L. Hudson, D. Y. Sasaki, R. P. Manginell, and C. C. Wong, "Microfabricated silicon gas chromatographic microchannels: Fabrication and performance," *Proc. SPIE*, vol. 3511, pp. 262–282, 1988.

- [4] E. J. Severin, B. J. Doleman, and N. S. Lewis, "An investigation of the concentration dependence and response to analyte mixtures of carbon black/insulating organic polymer composite vapor detectors," *Analyt. Chem.*, vol. 72, no. 4, pp. 658–668, 2000.
- [5] A. Heilig, N. Bârsan, U. Weimar, M. Schweizer-Berberich, J. W. Gardner, and W. Göpel, "Gas identification by modulating temperatures of SnO<sub>2</sub>-based thick film sensors," *Sens. Actuators B*, vol. 43, pp. 45–51, 1997.
- [6] E. Llobet, R. Ionescu, S. Al-Khalifa, J. Brezmes, X. Vilanova, X. Correig, N. Bârsan, and J. W. Gardner, "Multicomponent gas mixture analysis using a single tin oxide sensor and dynamic pattern recognition," *IEEE Sensors J.*, vol. 1, no. 3, pp. 207–213, 2001.
- [7] K. Ihokura and J. Watson, *The Stannic Oxide Gas Sensor, Principles and Applications*. Boca Raton, FL: CRC Press, 1994.
- [8] T. Iwaki, J. A. Covington, and J. W. Gardner, "Identification of vapours using a single carbon black/polymer composite sensor and a novel temperature modulation technique," *Proc. IEEE Sensors 2007*, pp. 1229–1232, Oct. 2007.
- [9] E. J. Severin, "Array based vapor sensing using conductive carbon black-polymer composite thin film detectors," Ph.D. dissertation, Dept. Mech. Eng., Calif. Inst. Technol., Pasadena, CA, 1999.
- [10] S. M. Briglin and N. S. Lewis, "Characterization of the temporal response profile of carbon black-polymer composite detectors to volatile organic vapors," *J. Phys. Chem. B*, vol. 107, pp. 11031–11042, 2003.
- [11] J. Crank, *The Mathematics of Diffusion*, 2nd ed. Bristol, U.K.: Oxford Univ. Press, 1975.
- [12] A. P. Prudnikov, Y. A. Brychkov, and O. I. Marichev, "Integrals and Series," vol. 1, Transl.: from Russian by N. M. Queen, Elementary functions.
- [13] E. J. Severin, "Array based vapor sensing using conductive carbon black-polymer composite thin film detectors," Ph.D. dissertation, Calif. Inst. Technol., Pasadena, CA, 1999.
- [14] T. Iwaki, J. A. Covington, J. W. Garder, F. Udrea, C. S. Blackman, and I. P. Parkin, "SOI-CMOS based single crystal silicon micro-heaters for gas sensors," *Proc. IEEE Sensors 2006*, pp. 460–463, Oct. 2006.
- [15] L. Pauling, *The Nature of the Chemical Bond*, 3rd ed. Ithaca, NY: Cornell Univ. Press, 1960.
- [16] BioDot, Inc., accessed Sep. 14, 2008. [Online]. Available: <http://www.biodot.com/>
- [17] N. C. Das, T. K. Chaki, and D. Khastgir, "Effect of processing parameters, applied pressure and temperature on the electrical resistivity of rubber-based conductive composites," *Carbon 40*, pp. 807–816, 2002.
- [18] D. R. Lide, *Handbook of Chemistry & Physics 2006–2007*, 87th ed. Boca Raton, FL: CRC Press, 2006.
- [19] Y. S. Kim and Y. S. Yang, "Additional thermodynamic feature extraction from chemoresistive carbon black-polymer composite sensors by temperature modulation," *Sens. Actuators B*, vol. 121, pp. 507–514, 2007.
- [20] E. Llobet, R. Ionescu, S. Al-Khalifa, J. Brezmes, X. Vilanova, X. Correig, and N. Bârsan, "Multicomponent gas mixture analysis using a single tin oxide sensor and dynamic pattern recognition," *IEEE Sensors J.*, vol. 1, no. 3, pp. 207–213, 2001.
- [21] A. Pike and J. W. Gardner, "Thermal modelling and characterisation of micropower chemoresistive silicon sensors," *Sens. Actuators B*, vol. 45, pp. 19–26, 1997.
- [22] T. Iwaki, J. A. Covington, F. Udrea, and J. W. Gardner, *Sens. Actuators B*, submitted to.



**Takao Iwaki** received the B.Sc. and M.Sc. degrees in physics from Tokyo University, Tokyo, Japan, in 1995 and 1997, respectively, and the Ph.D. degree in engineering from Warwick University, Coventry, U.K., in 2008.

He is with the Research Laboratories of Denso Corporation since 1997. His research interests include gas sensors and microsystem technology.

Dr. Iwaki is a member of the Institute of Electrical Engineers of Japan (IEEJ).



**James Covington** received the B.Eng., M.Res. (Masters of Research), and the Ph.D. degrees in 1996, 1997, and 2000, respectively, from the University of Warwick, Coventry, U.K. His Ph.D. was on the development of CMOS and SOI CMOS gas sensors for room temperature and high temperature operation.

He is presently an Associate Professor in the School of Engineering, University of Warwick, Coventry, U.K. He worked as a Research Fellow for both Warwick University and Cambridge University

on the development of gas and chemical sensors and was appointed as a Lecturer in 2002. Current research interests focus on the development of silicon devices with novel materials using CMOS and SOI ASIC technology (nose-on-a-chip), and biologically inspired neuromorphic devices with applications based on environmental and biomedical engineering.

Prof. Covington is a member of the Institute of Engineering and Technology (U.K.).



**Julian Gardner** (SM'87) received the B.Sc. from Birmingham University, Birmingham, U.K., Ph.D. from Cambridge University, U.K., and the D.Sc. degree from the Warwick University, Coventry, U.K.

He is a Professor of Electronic Engineering in the School of Engineering, Warwick University, Coventry, U.K. He is author or coauthor of over 400 technical papers and patents, as well as six technical books in the area of microsensors and machine olfaction. He is Series Editor for a books series by Wiley-VCH. He is a Fellow of the IEE

and has served on many advisory panels on sensors, e.g., for EPSRC, DTI, and IEE Professional Network on Microsystems and Nanotechnology. He has worked with over 20 companies in the past 15 years developing commercial e-nose instruments and a consultant for various companies. He is also Head of the Sensors Research Laboratory and Director of the Centre for Cognitive and Neural Systems. His research interests include the modeling of silicon microsensors, chemical sensor array devices, biomimetic MEMS devices, and electronic noses.

Dr. Gardner is a Fellow of the Institute of Engineering and Technology (U.K.) and was elected a Fellow of the Royal Academy of Engineering in 2006 and Awarded the J. J. Thomson Medal for Outstanding Achievement in Electronics by the Institute of Engineering and Technology in 2007.